

Non-linear evolution of GRE phase as a means to investigate tissue microstructure

F. Schweser^{1,2}, A. Deistung¹, D. GÜLLMAR¹, M. Atterbury^{1,3}, B. W. Lehr¹, K. Sommer^{1,4}, and J. R. Reichenbach¹

¹Medical Physics Group, Dept. of Diagnostic and Interventional Radiology 1, Jena University Hospital, Jena, Germany, ²School of Medicine, Friedrich Schiller University of Jena, Jena, Germany, ³Dept. of Physics, Brown University, Providence, RI, United States, ⁴School of Physics and Astronomy, Friedrich Schiller University of Jena, Jena, Germany

INTRODUCTION – Gradient-echo (GRE) magnetic resonance phase data are proportional to the magnetic field, providing useful information for several applications such as quantitative susceptibility mapping¹, or anatomical contrast analyses^{2,3}. However, the sources of the phase contrast and their relative contributions to the phase signal are still contentious. Recently, orientation dependent sources of phase signal have been discussed, namely the non-spherical Lorentzian cavity⁴ and anisotropic magnetic susceptibility^{5,6}. In this context, all experimental and theoretical investigations have hitherto relied on the linearity of the GRE phase with echo time (TE), or in other words, a time-invariant total Larmor frequency f of the voxel signal. In this contribution, we demonstrate and investigate the occurrence of non-linear phase evolution in the human brain.

MATERIALS & METHODS

Data Acquisition: Volunteer brain data were acquired with an interleaved multi-echo GRE sequence with 32 echoes and inter-echo spacing of 1.8 ms ($TE_i/TE_{32} = 4.6\text{ms}/62\text{ms}$, $TR/FA/BW_{1-32} = 67\text{ms}/15^\circ/391\text{Hz}/\text{px}$, voxel size $1.17 \times 1.17 \times 1.17 \text{ mm}^3$, 75% PF in phase and slice encoding direction) on a 3T MR-scanner (Tim Trio, Siemens Medical Solutions) using a 12-channel head-matrix coil. Orientation dependence of the contrast was investigated by performing the scan with the volunteer's head in two different positions with respect to the main magnetic field, in the normal head position and with the head tilted approximately -50° around the left-right axis. In order to determine whether the blood vessel network is involved in the non-linear contrast⁷ the scan was repeated in the normal position during Carboen (95% O_2 , 5% CO_2) inhalation, which modulated the venous signal. Finally, an EPI-DTI sequence was applied in the normal head position ($TE/TR/b\text{-value}/n\text{DiffDirections} = 91\text{ms}/6900\text{ms}/1000\text{s mm}^{-2}/76$, voxel size $2.5 \times 2.5 \times 2.5 \text{ mm}^3$).

Data Processing and Analysis: Based on diffusion tensor imaging (DTI) data maps of both fractional anisotropy (FA) and angles between the first Eigenvector (principal fiber orientation) and the external magnetic field were computed. Brain voxels with a fractional anisotropy below 0.3 were set to zero. Phase images were unwrapped using a 3D algorithm⁸. The constant B1-related phase offset was calculated¹ and subtracted from the phase images. The resulting images were divided by the corresponding TE_i resulting in Larmor frequency maps. These maps were further processed using the SHARP method¹ in order to remove background field contributions. The frequency image of the first echo (4.6 ms) was subtracted from all other phase images in order to obtain the temporal change of the frequency $\Delta f = f_{TE} - f_{4.6\text{ms}}$, and 6th-order polynomial fitting was applied to eliminate low frequency variations. Finally, all images were registered to the DTI dataset using FLIRT⁹. Averaged magnitude and frequency values were obtained for all echoes in volumes of interest (VOIs) (not shown) located in the optic radiation and adjacent white matter (WM) parenchyma (less non-linear effects; see Results section) of the normal head position data, respectively. Both a one- and a two-compartment complex-valued signal model were fitted to the time-courses of magnitude and frequency in these VOIs.

RESULTS – Figure 1 depicts representative slices of the frequency maps (Fig. 1a,b), frequency change (Fig. 1d,e), and DTI information (third row) for air inhalation. The differences induced by Carboen inhalation (with respect to air inhalation) are shown for the frequency and frequency change in Figs. 1c and 1f, respectively. The frequency maps (Fig. 1a,b) demonstrate considerable different contrast depending on the orientation of the head, as reported previously¹. Inhalation of Carboen did only change the frequency measured in venous vessels and adjacent to them (arrows in Fig. 1c). The frequency change at $TE=21\text{ms}$ (with respect to the 4.6 ms echo) is negative and depends on the orientation of the head (arrows in Fig. 1d,e). Carboen inhalation had no effect on the frequency change (Fig. 1f). The frequency change is most prominent in WM regions with high FA (Fig. 1i) and medium to high angles between fibers and magnetic field (arrows in Fig. 1g,h). The mean magnitude and frequency-difference in both optic radiation and WM are shown as a function of echo time in Fig. 2. In WM, 99% of the signal was attributed to tissue with an R_2^* of 21 Hz and a frequency difference of -25 Hz was found between the two compartments (dotted blue lines in Fig. 2). In the optic radiation, 83% was attributed to tissue with $R_2^*=17$ Hz, while 17% was attributed to a compartment with $R_2^*=114$ Hz and a frequency difference of 12 Hz (dotted black lines in Fig. 2). The one-compartment fit did not describe the data sufficiently (straight red lines in Fig. 2).

DISCUSSION & CONCLUSIONS – The non-linear phase evolution was demonstrated to be orientation dependent (Fig. 1d,e) and restricted to regions with high FA (Fig. 1i), and seems to be related to high angles between fibers and magnetic field (approx. $>30^\circ$, Fig. 1g,h). Furthermore, the non-linearity is independent from the venous blood vessel network (Fig. 1c) and has a significant contribution (approx. 1–1.5 Hz) to the overall phase contrast at echo times usually applied in phase imaging studies² ($TE > 20$ ms at 3 T). In the optic radiation, a two-compartment signal model with different Larmor frequencies and relaxation rates could describe the observed effect (dotted black lines in Fig. 2). While the relaxation rate of the larger compartment (17 Hz) was similar to the value determined previously for WM, e.g., by Peters et al.¹⁰ (19 Hz), the value of the smaller compartment (114 Hz) is consistent with a recent preliminary observation by Lenz et al.¹¹, who attributed this second compartment to the myelin water fraction. In normal WM parenchyma (less non-linear effects) the relaxation rate of the larger compartment was slightly higher (21 Hz) than determined by Peters et al.¹⁰, but the second compartment contributed only 1% to the total signal. The physical origin of the relaxation, however, remains unclear. It can be explained by both, the non-spherical Lorentzian cavity model³ and simple magnetic susceptibility effects on the myelin water fraction which is enclosed by the tubular (potentially diamagnetic) myelin sheets. More detailed analyses will be performed in future including correlation of non-linear phase effects with fiber orientation from DTI data.

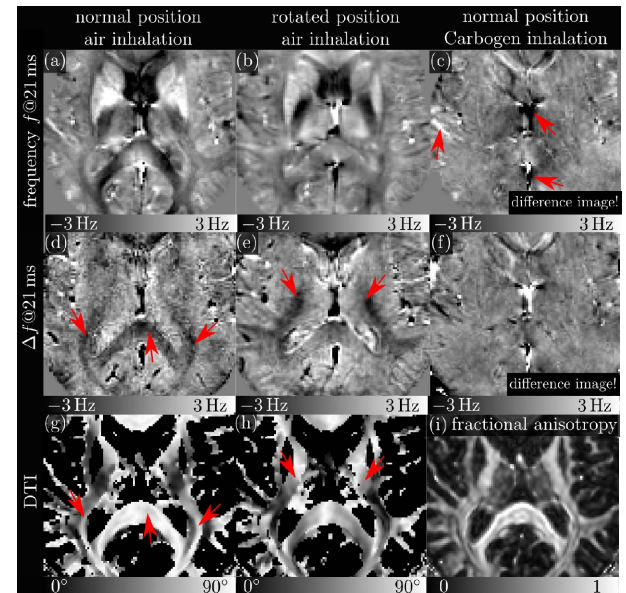


FIGURE 1. Frequency maps (a,b) and frequency change maps (d,e) of the $TE_9=21\text{ms}$ echo in normal head position (left column) and rotated head (middle column) with air inhalation. The differences between air and Carboen inhalation are shown in the right column for the frequency map (c) and frequency change (f). Fiber directions and FA are shown in (g,h) and (i), respectively.

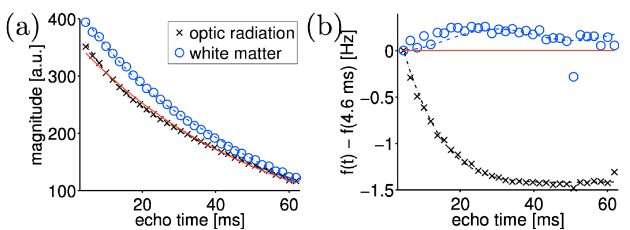


FIGURE 2. Time-course of magnitude (a) and frequency change (b) of VOIs in optic radiation and WM. The dashed blue and black lines indicate the two-compartment fits. The straight red line is the one-compartment fit to the region of the optic radiation.

REFERENCES – [1] Schweser F, et al. *NeuroImage*. 2010; [2] Duyn J, et al. *PNAS*. 2007;104(28):11796-801. [3] Deistung et al. *Magn Reson Med*. 2008;60(5):1155-68. [4] He Y and Yablonskiy DA. *PNAS*. 2009;106(32):13558-63. [5] Liu C. *Magn Reson Med*. 2010;63(6):1471-7. [6] Lee J, et al. *PNAS*. 2010;107(11):5130-5. [7] Sukstanskii AL and Yablonskiy DA. *J Magn Reson*. 2001;151(1):107-17. [8] Abdul-Rahman HS, et al. *Appl Opt*. 2007;46(26):6623-3. [9] Jenkinson M, et al. *NeuroImage*. 2002;17(2):825-41. [10] Peters A, et al. *Magn Reson Med*. 2007;25(6):748-53. [11] Lenz C, et al. *ISMRM*, p676, 2010.